

Magnetic Fluid Based Squeeze Film in Rough Rotating Curved Porous Annular Plates: Deformation Effect

M. E. Shimpi, G. M. Deheri

Abstract—This article aims to investigate the performance of a magnetic fluid based squeeze film between rotating transversely rough curved porous annular plates incorporating the effect of elastic deformation. The associated stochastically averaged Reynolds type equation is solved to obtain the pressure distribution leading to the calculation of the load carrying capacity. The results suggest that the transverse roughness of the bearing surfaces affects the performance adversely although the bearing systems register a relatively improved performance due to the magnetization. The deformation causes reduced the load carrying capacity while the curvature parameters tend to nominally increase the load carrying capacity. Besides, the adverse effect of porosity, deformation and standard deviation can be minimized to some extent by the positive effect of the magnetization and the curvature parameters in the case of negatively skewed roughness by suitably choosing the rotational inertia and the aspect ratio, which becomes significant when negative variance occurs.

Keywords—Annular plates curved rough surface, deformation, load carrying capacity, rotational inertia, magnetic fluid, squeeze film.

I. INTRODUCTION

THE behavior of squeeze film between various geometrical configurations of the flat surface was analyzed by Archibald [1]. Wu [2], [3] investigated the performance of the squeeze film for porous annular disks and rotating porous annular disks respectively. Ting [4] simplified the method of Wu [2], [3] considerably by taking only the lower disk to be rotating. Prakash and Vij [5] resorted to the well known Morgan Cameron approximation when the porous facing thickness was assumed small. In fact, they considered squeeze film in porous plates of various geometries. Hays [6] discussed the squeeze film phenomenon between the curved plates considering the curvature of sine form keeping minimum film thickness as constant. Murti [7] dealt with the squeeze film performance in curved circular plates describing the film thickness by an exponential expression. His analysis was based on the assumption that the central film thickness was constant instead of minimum film thickness as considered by Hays [6]. Gupta and Vora [8] discussed the corresponding problem for annular plates. In the above analysis only the lower plate was flat. Ajwalya [9] developed this analysis by assuming the lower plate also to be curved. According to his

findings such situation could be found useful in the design of machine elements like clutch plates and collar bearings. Patel and Deheri [10] studied the behavior of squeeze film between curved circular plates describing the film thickness by a hyperbolic expression.

All the above studies dealt with conventional lubricants. Use of magnetic fluid as a lubricant modifying the performance of the bearing system has attracted considerable attentions. Verma [11] investigated the squeeze film performance by taking a magnetic fluid lubricant. Bhat and Deheri [12] extended the above analysis to present a study of the squeeze film performance in porous annular disks in the presence of a magnetic fluid lubricant. Here it was found that the application of magnetic fluid lubricant improved the performance of the squeeze film. The magnetic fluid consisted of fine magnetic grains suspended in a magnetically passive solvent. Regarding the details of the behavior and properties of magnetic fluid one can turn to Bhat [13]. However, in actual practice the flatness of the plates does not endure due to elastic, thermal and uneven wear effects. With this point of view, Bhat and Deheri [14] investigated the performance of magnetic fluid based squeeze film on the configuration of Ajwalya [9]. Patel and Deheri [15] considered the squeeze film behaviour between curved circular plates lying along the surface determined by a secant function under the presence of a magnetic fluid lubricant. Here it was found that the magnetic fluid lubricant significantly enhanced the performance of the bearing system. Lin, Lu and Liao [16] dealt with the squeeze film performance between the curved circular plates with an electrically conducting fluid in the presence of a transverse magnetic field.

The bearings surfaces particularly, after receiving some run-in and wear develop roughness. Even sometimes contamination of lubricants and chemical degradation of the surfaces add to roughness. The roughness appears to be random in character seldom following any particular structural pattern.

In order to study and analyze the effect of surface roughness on the performance of bearing system several methods have been proposed. A stochastic approach to mathematically model the random roughness was adopted by [17]-[20]. A comprehensive general analysis for the surface roughness (both transverse as well as longitudinal) based on a general probability density function was deployed by Christensen and Tonder [18]-[20] by developing the approach of Tzeng and Seibel [17]. Subsequently, a good number of investigations

M. E. Shimpi is with the Birla Vishvakarma Mahavidyalaya Engineering College, Vallabh Vidyanagar, Anand, Gujarat, India (corresponding author phone: 02692-239847; e-mail: mukesh.shimpi@gmail.com).

G.M. Deheri is with the Sardar Patel University, Vallabh Vidyanagar, Anand, Gujarat, India (e-mail: gm.deheri@rediffmail.com).

$$f(h) = (h + p' p_a \delta)^3 + 3(\alpha^2 + \sigma^2)(h + p' p_a \delta) + 3\sigma^2 \alpha + \alpha^3 + \varepsilon \quad (10)$$

where

$$H^2 = k(r-a)(b-r); \quad (11)$$

$$h = h_0 \left[1 + \frac{1}{1+Br} - \frac{1}{1+Cr} \right], \quad a < r < b \quad (12)$$

where $k = 10^{14} A^2 m^{-4}$ chosen so as to have a magnetic field of strength over $k = 10^5$ [Bhat [13]], μ_0 is permeability of free space, $\bar{\mu}$ is the magnetic susceptibility of particles and μ is the viscosity of the lubricant, ϕ is the permeability of porous facing, H_0 is the thickness of porous medium, δ is the local elastic deformation of the porous facing, p_a is the reference ambient pressure.

The concerned boundary conditions are

$$p(a) = 0, \quad p(b) = 0 \quad (13)$$

In view of the following non-dimensional quantities,

$$\begin{aligned} P &= -\frac{h_0^3 p}{\mu \dot{h}(b^2 - a^2)}, \quad R = \frac{r}{a}, \quad \bar{\sigma} = \frac{\sigma}{h_0}, \quad \bar{\alpha} = \frac{\alpha}{h_0}, \\ \bar{\varepsilon} &= \frac{\varepsilon}{h_0^3}, \quad \bar{\psi} = \frac{\phi H_0}{h_0^3}, \quad \bar{\kappa} = \frac{12\mu \dot{h}}{h_0^3}, \quad \bar{\mu}^* = -\frac{\mu_0 \bar{\mu} k h_0^3}{\mu \dot{h}}, \\ \bar{B} &= Br, \quad \bar{C} = Cr, \quad \bar{p} = p' p_a, \quad \bar{\delta} = \frac{\delta}{h}, \quad m = \frac{b}{a}, \quad s = \frac{3\rho\Omega^3}{p_a} \end{aligned} \quad (14)$$

(ρ being density of lubricant and Ω is angular velocity)

Integrating the stochastically averaged Reynolds equation under the boundary conditions (13) one obtains the expression for the non-dimensional pressure distribution

$$\begin{aligned} P &= \frac{0.5\bar{\mu}^* (R-1)(m-R)}{m^2-1} - \frac{6}{m^2-1} \left[\frac{D_2}{A_3} (R-1) + \frac{X}{Z} \log R \right] \\ &\quad - \frac{6}{m^2-1} \left[\lambda_1 - \frac{X}{2Z} \right] \log \left(\frac{A_1 + A_2 R + A_3 R^2}{A_1 + A_2 + A_3} \right) \\ &\quad - \frac{6}{m^2-1} \left[\lambda_2 - \frac{XA_2}{Z\sqrt{4A_1 A_3 - A_2^2}} \right] \times \\ &\quad \left[\tan^{-1} \left(\frac{2A_3 R + A_2}{\sqrt{4A_1 A_3 - A_2^2}} \right) - \tan^{-1} \left(\frac{2A_3 + A_2}{\sqrt{4A_1 A_3 - A_2^2}} \right) \right] \end{aligned} \quad (15)$$

where

$$\begin{aligned} A_1 &= 1 + 3\bar{p} \bar{\delta} + 3(\bar{p} \bar{\delta})^2 + 3\bar{\alpha}(1 + \bar{p} \bar{\delta})^2 \\ &\quad + 3(\bar{\alpha}^2 + \bar{\sigma}^2)(1 + \bar{p} \bar{\delta}) + 3\bar{\sigma}^2 \bar{\alpha} + \bar{\alpha}^3 + \bar{\varepsilon} + 12\bar{\psi} \end{aligned} \quad (16)$$

$$\begin{aligned} A_2 &= 3(\bar{C} - \bar{B}) \left[1 + 3\bar{p} \bar{\delta} + 3(\bar{p} \bar{\delta})^2 \right. \\ &\quad \left. + 2\bar{\alpha}(1 + \bar{p} \bar{\delta})^2 + 3(\bar{\alpha}^2 + \bar{\sigma}^2)(1 + \bar{p} \bar{\delta}) \right] \end{aligned} \quad (17)$$

$$A_3 = 3(\bar{C} - \bar{B})^2 \left[1 + 3\bar{p} \bar{\delta} + 3(\bar{p} \bar{\delta})^2 + \bar{\alpha}(1 + \bar{p} \bar{\delta})^2 \right] \quad (18)$$

$$\begin{aligned} B_1 &= 1 + 3\bar{p} \bar{\delta} + 3(\bar{p} \bar{\delta})^2 \\ &\quad + 3(\bar{\alpha}^2 + \bar{\sigma}^2)(1 + \bar{p} \bar{\delta}) + 3\bar{\sigma}^2 \bar{\alpha} + \bar{\alpha}^3 + \bar{\varepsilon} \end{aligned} \quad (19)$$

$$B_2 = 3(\bar{C} - \bar{B}) \left[1 + 3\bar{p} \bar{\delta} + 3(\bar{p} \bar{\delta})^2 + 3(\bar{\alpha}^2 + \bar{\sigma}^2)(1 + \bar{p} \bar{\delta}) \right] \quad (20)$$

$$D_1 = 1 + 4B_1 (s/\kappa); \quad (21)$$

$$D_2 = \left(\frac{8}{3} \right) B_2 (s/\kappa); \quad (22)$$

$$\lambda_1 = \frac{A_3 D_1 - A_2 D_2}{2A_3^2}; \quad (23)$$

$$\lambda_2 = \frac{2A_1 A_3 D_2 - A_2 (A_3 D_1 - A_2 D_2)}{A_3^2 \sqrt{4A_1 A_3 - A_2^2}}; \quad (24)$$

$$\begin{aligned} X &= \frac{D_2}{A_3} (m-1) + \lambda_1 \log \left[\frac{A_1 + A_2 m + A_3 m^2}{A_1 + A_2 + A_3} \right] \\ &\quad + \lambda_2 \left[\tan^{-1} \left(\frac{2A_3 m + A_2}{\sqrt{4A_1 A_3 - A_2^2}} \right) - \tan^{-1} \left(\frac{2A_3 + A_2}{\sqrt{4A_1 A_3 - A_2^2}} \right) \right] \end{aligned} \quad (25)$$

$$\begin{aligned} Z &= -\log(m) + \frac{1}{2} \log \left[\frac{A_1 + A_2 m + A_3 m^2}{A_1 + A_2 + A_3} \right] + \\ &\quad \frac{A_2}{\sqrt{4A_1 A_3 - A_2^2}} \left[\tan^{-1} \left(\frac{2A_3 m + A_2}{\sqrt{4A_1 A_3 - A_2^2}} \right) - \tan^{-1} \left(\frac{2A_3 + A_2}{\sqrt{4A_1 A_3 - A_2^2}} \right) \right] \end{aligned} \quad (26)$$

The load carrying capacity in non-dimension form then, is derived as

$$W = -\frac{h_0^3 w}{\mu \dot{h}(b^2 - a^2)^2} = \frac{2\pi}{m^2-1} \int_1^m R P dR \quad (27)$$

which turns out to be

$$\begin{aligned} W &= 2\pi \left[\frac{\bar{\mu}^*}{24} \left(\frac{m-1}{m+1} \right) - \frac{D_2 (2m+1)}{A_2 (m+1)^2} - \right. \\ &\quad \left. \frac{3X}{Z} \frac{m^2 \log m}{(m^2-1)^2} + \frac{3\lambda_1}{m^2-1} + \frac{1.5E_1 E_2 (m-1)}{(m^2-1)^2} \right] \end{aligned}$$

$$\begin{aligned}
& -\frac{3}{(m^2-1)^2} \left[\frac{E_1 E_2}{4A_3} + \frac{E_3 (A_3 m^2 + A_2)}{A_3} \right] \log \left(\frac{A_1 + A_2 m + A_3 m^2}{A_1 + A_2 + A_3} \right) \\
& + \frac{3}{(m^2-1)^2} \left[E_1 \left(1 + \frac{2A_1 A_3 - A_2^2}{4A_3^2} \right) + 2E_3 E_4 \right] \tan^{-1} \left(\frac{2A_3 + A_2}{\sqrt{4A_1 A_3 - A_2^2}} \right) \\
& - \frac{3}{(m^2-1)^2} \left[E_1 \left(m^2 + \frac{2A_1 A_3 - A_2^2}{4A_3^2} \right) + 2E_3 E_4 \right] \tan^{-1} \left(\frac{2A_3 m + A_2}{\sqrt{4A_1 A_3 - A_2^2}} \right)
\end{aligned} \quad (28)$$

where,

$$E_1 = \lambda_2 - \frac{XA_2}{Z\sqrt{4A_1 A_3 - A_2^2}}; \quad (29)$$

$$E_2 = \frac{\sqrt{4A_1 A_3 - A_2^2}}{A_2}; \quad (30)$$

$$E_3 = \lambda_1 - \frac{X}{2Z}; \quad (31)$$

$$E_4 = \frac{2A_1 A_3 - A_2^2}{\sqrt{4A_1 A_3 - A_2^2}}. \quad (32)$$

III. RESULTS AND DISCUSSION

It can be easily seen that the dimensionless pressure distribution is obtained from (15) while the load carrying capacity in non-dimensional form is governed by (28). These two equations indicate that the dimensionless film pressure and load carrying capacity depend on various parameters such as μ^* , $\bar{\sigma}$, $\bar{\alpha}$, $\bar{\varepsilon}$, m , ψ , \bar{C} , \bar{B} , s/κ and $\bar{\delta}$. These parameters respectively describe the effect of magnetic fluid lubricant, surface roughness, aspect ratio, porosity, curvature parameters, rotational inertia and elastic deformation. A cursory glance at (28) suggests that the expression is linear in μ^* , as a result of which increasing values of μ^* would lead to increased load carrying capacity. It is found that for a nonporous bearing with smooth surfaces this study reduces to the investigation of Bhat and Deheri [12] dealing with magnetic fluid based squeeze film between annular plates in the absence of rotation and deformation. Further, setting the magnetization parameter μ^* to be equal to zero for a nonporous bearing with smooth surfaces one obtains the results of Prakash and Vij [5] in the absence of rotation and deformation. A closer look at (28) suggests that the elastic deformation of the bearing decreases the load carrying capacity. It is noticed from (15) that the non-dimensional pressure increases by

$$\frac{\mu^*}{2} \left[\frac{(R-1)(m-R)}{m^2-1} \right] \quad (33)$$

while (28) reveals that the dimensionless load carrying capacity enhances by

as compared to the case of conventional lubricant. Further, it is manifest that the aspect ratio plays a key role in improving the performance of magnetic fluid based bearing system. In addition, this (3) underlines that the elastic deformation of the bearing significantly distorts the profile of the pressure distribution.

It is noticed that the effect of transverse roughness is adverse in general and this negative effect gets further boosted due to elastic deformation. Probably, this is due to the fact that the roughness of the bearing surfaces retards the motion of lubricant, resulting in decreased lubricant pressure in turn, which leads to decreased load carrying capacity.

The variation of load carrying capacity with respect to the magnetization parameter for various values of $\bar{\sigma}$, $\bar{\alpha}$, $\bar{\varepsilon}$, m , ψ , \bar{C} , \bar{B} , s/κ and $\bar{\delta}$ presented in Figs 2-10 makes it clear that the load carrying capacity increases due to magnetic fluid lubricant. Therefore, it becomes clear from these graphs that the performance of bearing systems gets improved due to the magnetization and this positive effect is sharper in the case of standard deviation especially when negatively skewed roughness is involved. It is seen that the curvature parameters increase the load carrying capacity.

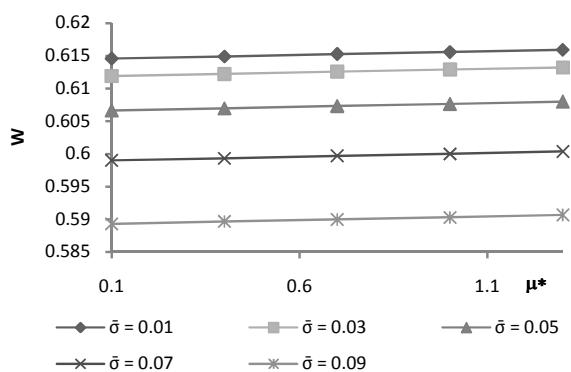
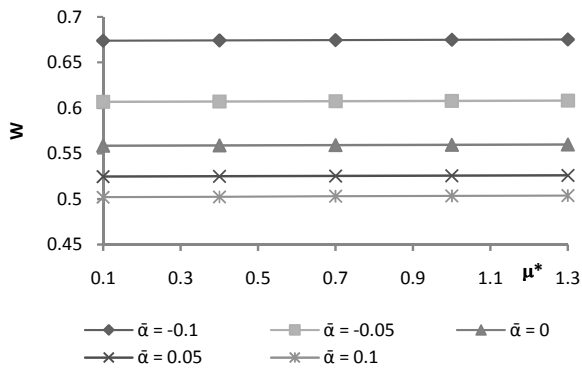
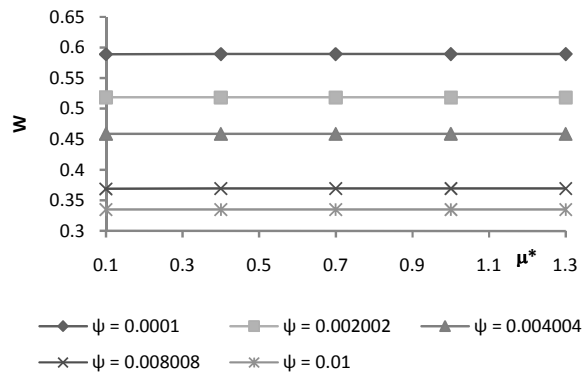
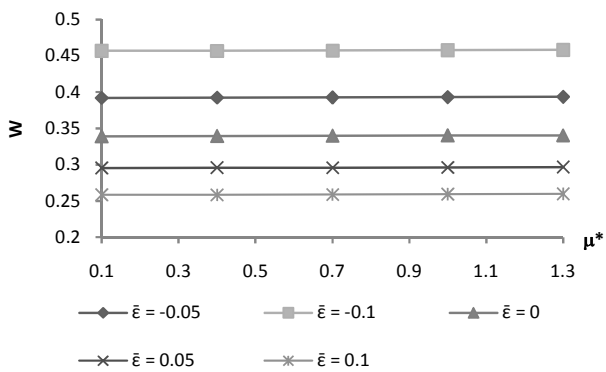
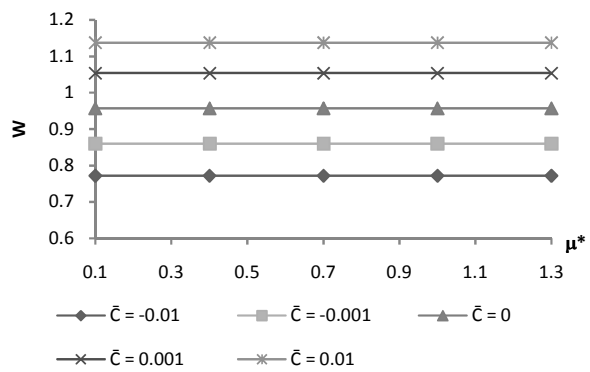
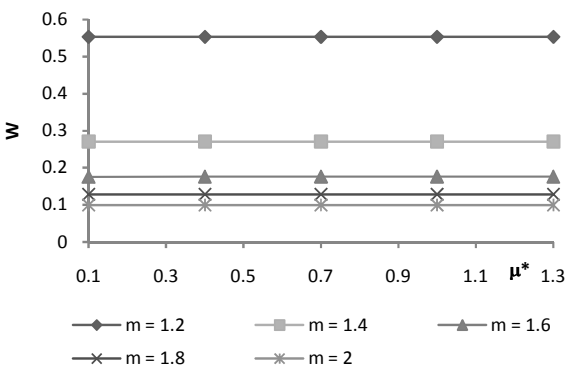
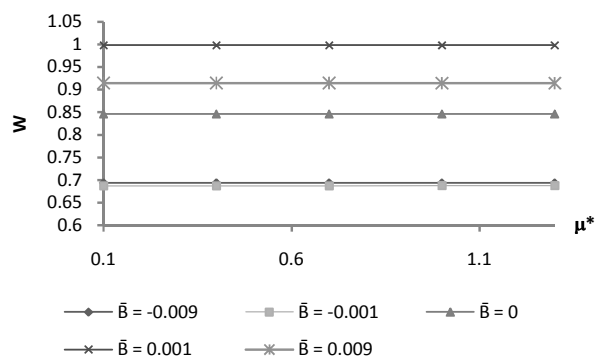


Fig. 2 Variation of Load carrying capacity with respect to μ^* and $\bar{\sigma}$


 Fig. 3 Variation of Load carrying capacity with respect to μ^* and $\bar{\alpha}$

 Fig. 6 Variation of Load carrying capacity with respect to μ^* and ψ

 Fig. 4 Variation of Load carrying capacity with respect to μ^* and $\bar{\varepsilon}$

 Fig. 7 Variation of Load carrying capacity with respect to μ^* and \bar{C}

 Fig. 5 Variation of Load carrying capacity with respect to μ^* and m

 Fig. 8 Variation of Load carrying capacity with respect to μ^* and \bar{B}

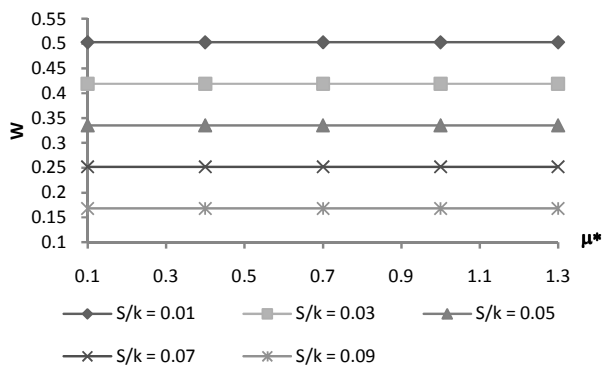


Fig. 9 Variation of Load carrying capacity with respect to μ^* and s/κ

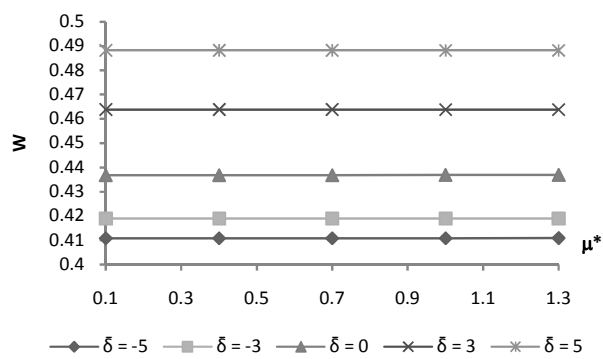


Fig. 10 Variation of Load carrying capacity with respect to μ^* and δ

Figs. 11-16 present the profile for the distribution of non-dimensional load carrying capacity with respect to the standard deviation associated with roughness. It is clearly noticed that the standard deviation adversely affects the bearing systems in the sense that the load carrying capacity decreases considerably due to the standard deviation. However, this decrease in load carrying capacity is relatively less in the case of the aspect ratio while this rate of decrease is more in the case of deformation. It is further seen that the decreased load carrying capacity due to the standard deviation gets further decreased owing to porosity.

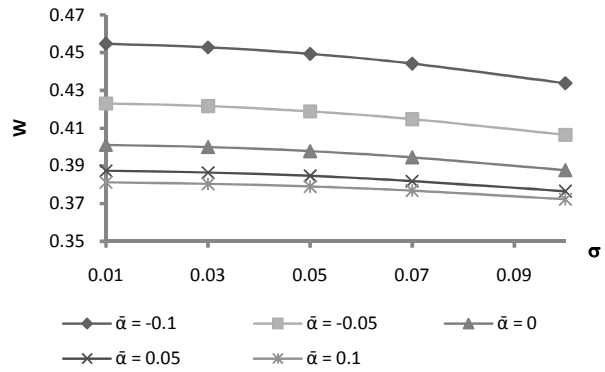


Fig. 11 Variation of Load carrying capacity with respect to σ and α

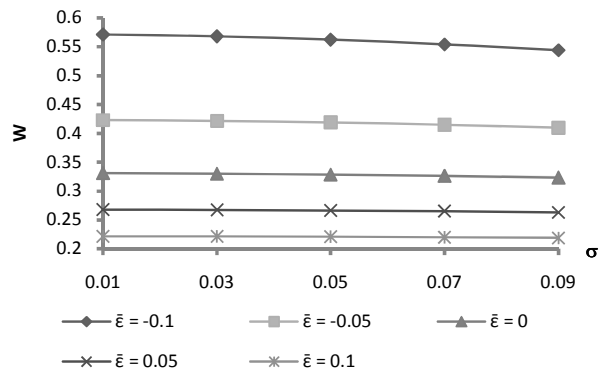


Fig. 12 Variation of Load carrying capacity with respect to σ and ϵ

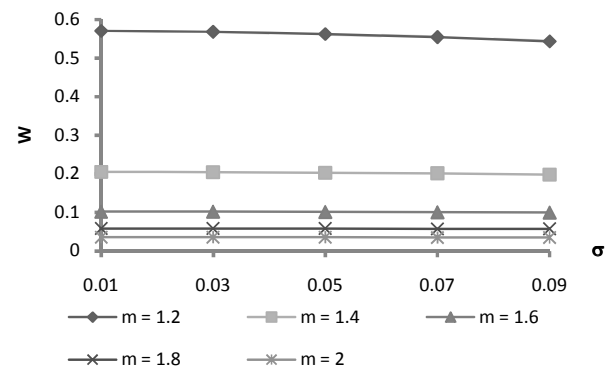


Fig. 13 Variation of Load carrying capacity with respect to σ and m

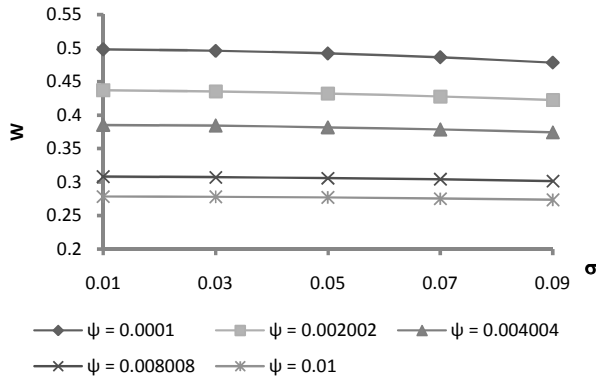


Fig. 14 Variation of Load carrying capacity with respect to $\bar{\sigma}$ and ψ

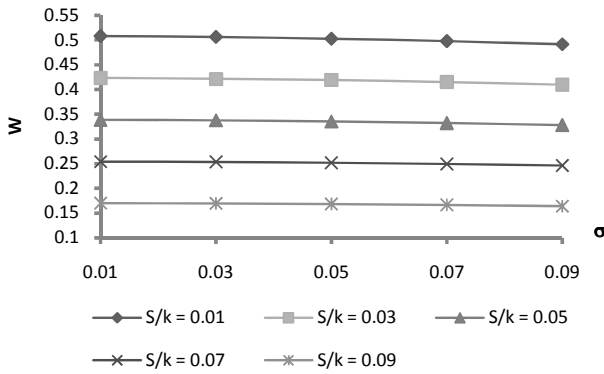


Fig. 15 Variation of Load carrying capacity with respect to $\bar{\sigma}$ and S/κ

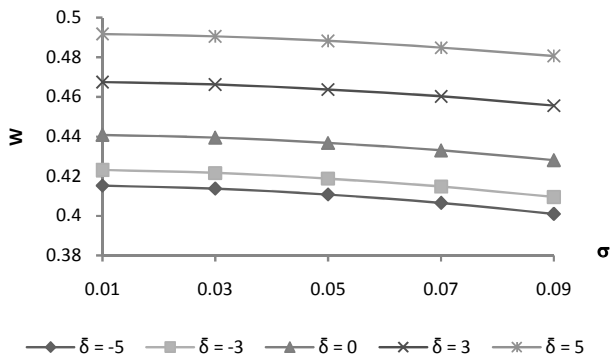


Fig. 16 Variation of Load carrying capacity with respect to $\bar{\sigma}$ and $\bar{\delta}$

In Figs 17-21, one can have the profile for the load carrying capacity with respect to $\bar{\alpha}$. It is seen that $\bar{\alpha}$ (positive) decreases the load carrying capacity while $\bar{\alpha}$ (negative) tends to increase the load carrying capacity except in the case of deformation where the trends are reversed.

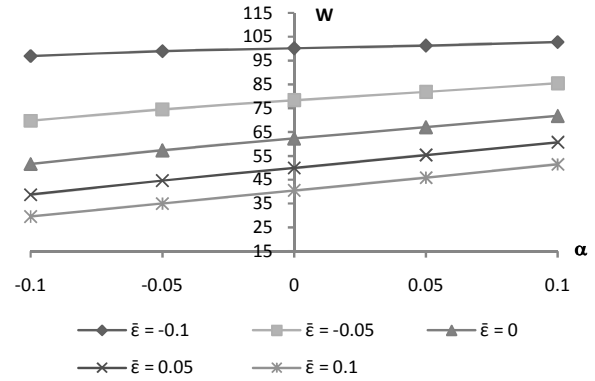


Fig. 17 Variation of Load carrying capacity with respect to $\bar{\alpha}$ and $\bar{\epsilon}$

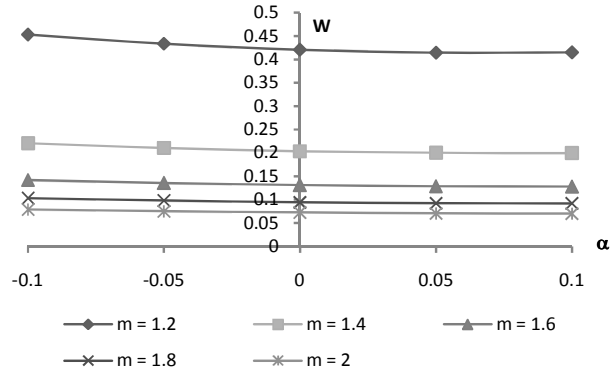


Fig. 18 Variation of Load carrying capacity with respect to $\bar{\alpha}$ and m

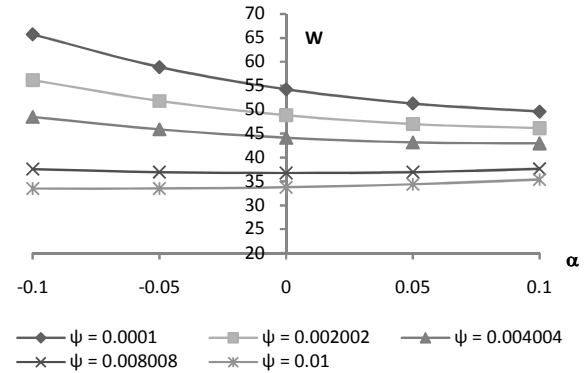
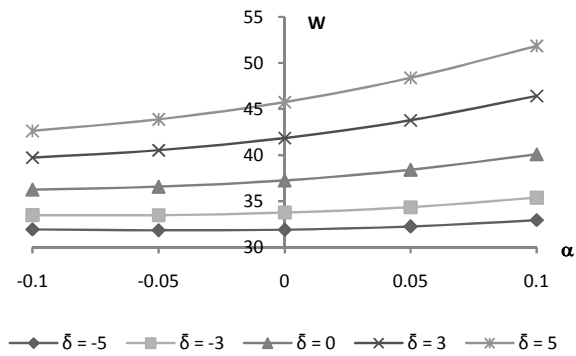
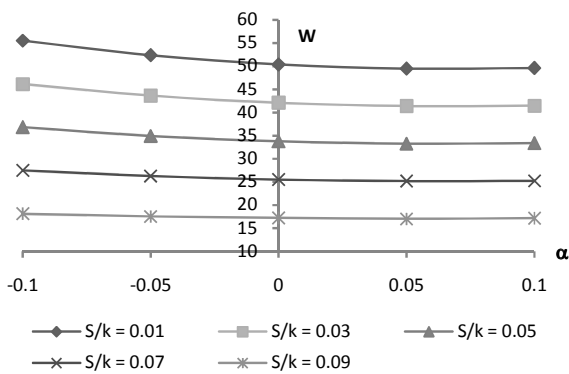
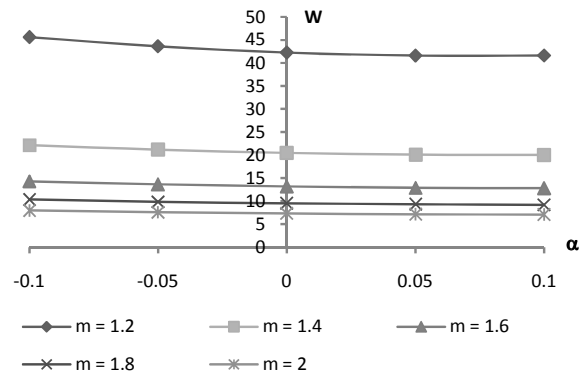
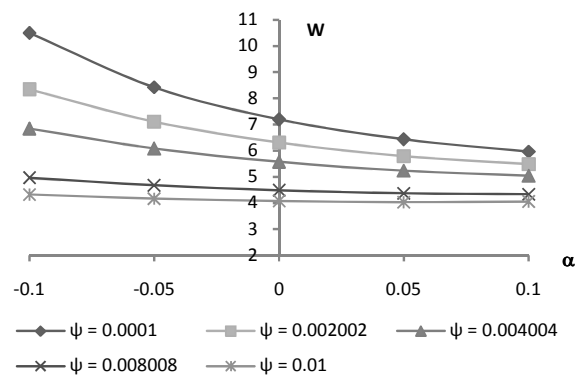
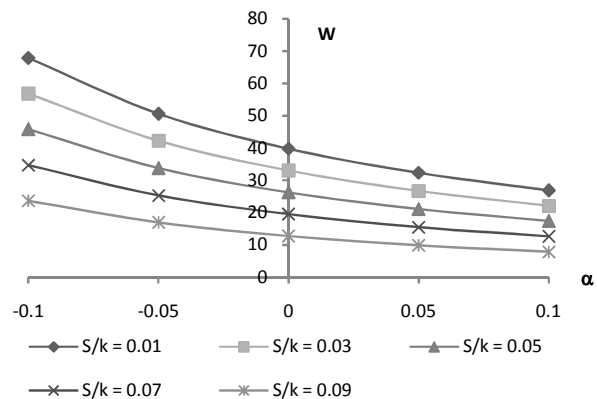
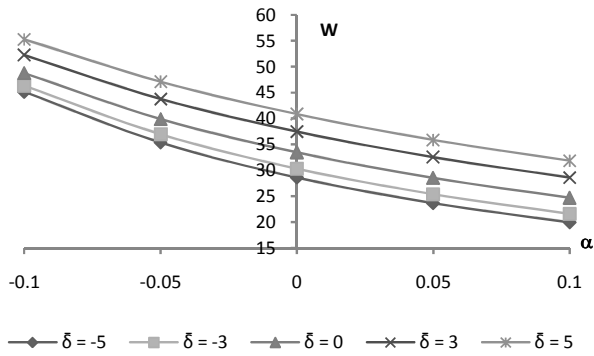


Fig. 19 Variation of Load carrying capacity with respect to $\bar{\alpha}$ and ψ

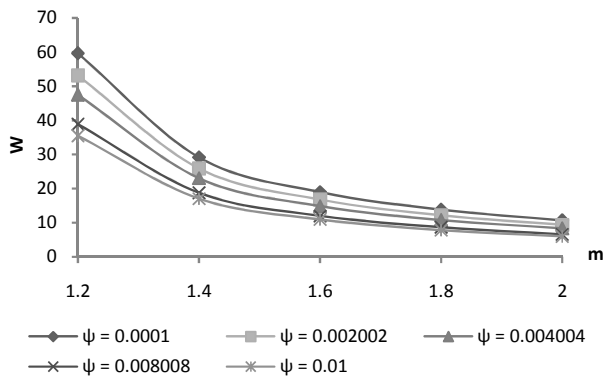
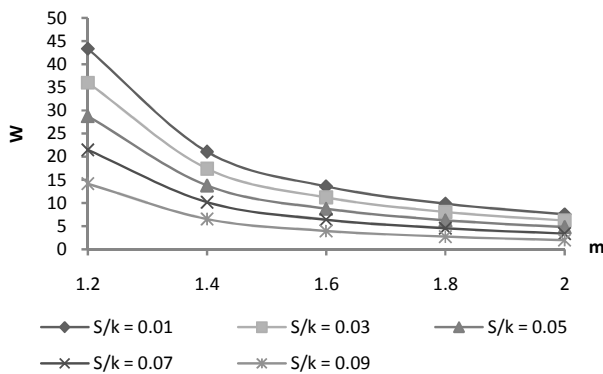
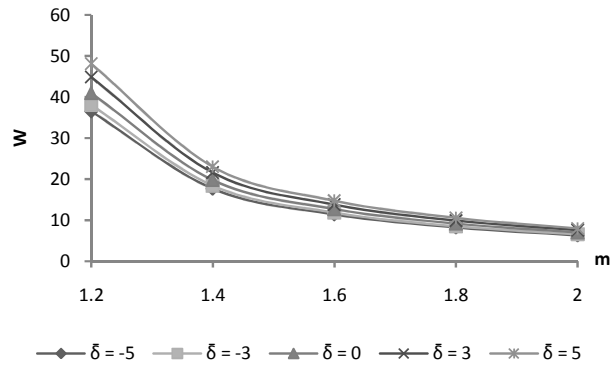
Fig. 20 Variation of Load carrying capacity with respect to $\bar{\alpha}$ and $\bar{\delta}$ Fig. 21 Variation of Load carrying capacity with respect to $\bar{\alpha}$ and S/κ

The variation of load carrying capacity with respect to skewness depicted in Figs 22-25 indicates that the trends skewness are identical with that of trends of $\bar{\alpha}$ except in the case of $\bar{\delta}$ wherein trends are opposite. Therefore, the combined effect of negatively skewed roughness and negative variance is significantly positive in most of the situations. Further, it is observed that the positive effect of negatively skewed roughness is quite sharp as compared to the positive effect of negative variance.

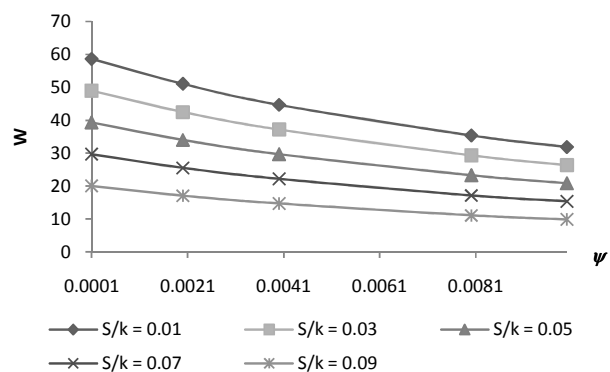
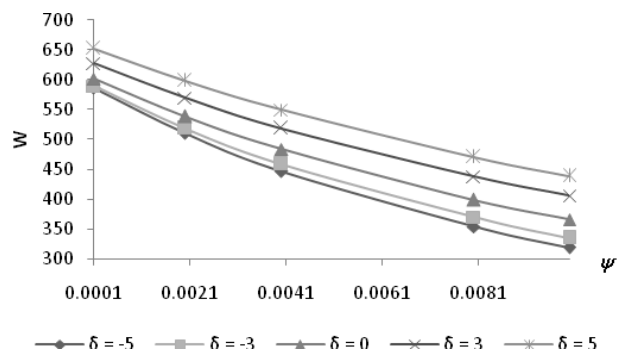
Fig. 22 Variation of Load carrying capacity with respect to $\bar{\varepsilon}$ and m Fig. 23 Variation of Load carrying capacity with respect to $\bar{\varepsilon}$ and ψ Fig. 24 Variation of Load carrying capacity with respect to $\bar{\varepsilon}$ and S/κ

Fig. 25 Variation of Load carrying capacity with respect to $\bar{\epsilon}$ and $\bar{\delta}$

The effect of the aspect ratio on the distribution of load carrying capacity presented in Figs 26-28 suggests that the aspect ratio has a strong effect on the performance of bearing system. In fact, the load carrying capacity decreases sharply with the increase in the aspect ratio.

Fig. 26 Variation of Load carrying capacity with respect to m and ψ Fig. 27 Variation of Load carrying capacity with respect to m and s/κ Fig. 28 Variation of Load carrying capacity with respect to m and $\bar{\delta}$

The effect of porosity on the distribution of load carrying capacity is considerably adverse as can be seen from Figs 29-30. One can see that indeed the load carrying capacity sharply decreases due to porosity and this effect is sharper in the case of deformation. Fig. 31 underlines that the rotational inertia s/κ decreases the load carrying capacity substantially and this decrease is more when a larger value of deformation is involved.

Fig. 29 Variation of Load carrying capacity with respect to ψ and s/κ Fig. 30 Variation of Load carrying capacity with respect to ψ and $\bar{\delta}$

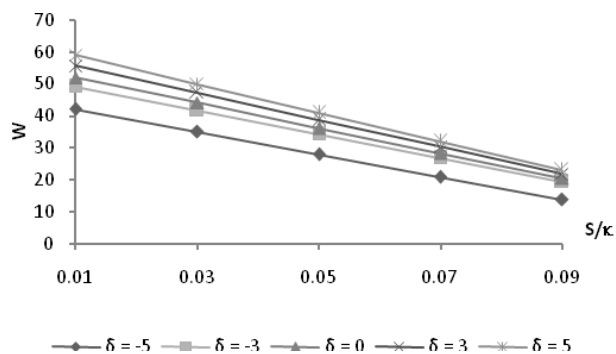


Fig. 31 Variation of Load carrying capacity with respect to s/κ and $\bar{\delta}$

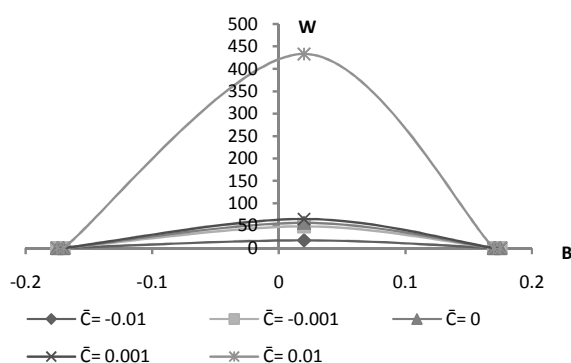


Fig. 32 Variation of Load carrying capacity with respect to \bar{B} and \bar{C}

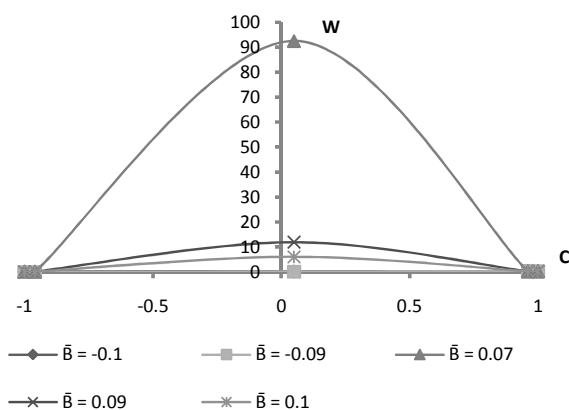


Fig. 33 Variation of Load carrying capacity with respect to \bar{C} and \bar{B}

Some of the figures presented here reveal that the combined negative effect of s/κ , m and ψ is more pronounced especially when larger values of deformation is involved.

Furthermore, the combined negative effect of porosity, deformation and rotational inertia can be compensated up to some extent by the positive effect of the magnetic fluid

lubricant in the case of negatively skewed roughness especially when negative variance is involved by choosing suitable values of aspect ratio.

From this investigation it is noticed that the effect of deformation becomes more significant when larger values of rotational inertia are involved. However, the effect of standard deviation remains adverse for a large range of values of deformation.

The results found here are in good agreement with various other earlier investigations Bhat and Deheri [14] and Deheri, Patel and Abhangi [33]. Some of the conclusions obtained here are in consonance with the results of Deheri, Patel and Abhangi [33] especially when the exponent shape is considered but for small range of curvature parameters, our study offers a slightly better measure in the case of secant shape. This article offers some measures for mitigating the adverse effect of porosity and roughness by the magnetic fluid lubricant for a squeeze film in rotating annular plates even if the bearing is deformed considerably. Of course, here the aspect ratio plays a crucial role in minimizing this adverse effect.

III. CONCLUSION

It is observed that most of the parameter appears to have adverse effect on the performance of the bearing system. However, the situation is retrieved up to certain extent by the positive effect of the magnetization and curvature parameters in the case of negatively skewed roughness. This study establishes that the bearing can support a load even when there is no flow. This article makes it mandatory that the roughness must be duly respected while designing this type of bearing system even if suitable values of curvature parameters and the aspect ratio are chosen. This is all the more essential from bearing's life period point of view. This investigation also underlines the importance of the curvature parameters in this type of rotating bearing system.

REFERENCES

- [1] F. R. Archibald, "Load Capacity and Time Relations for Squeeze Films", *Trans. ASME*, vol. 78, pp. A 231-245, 1956.
- [2] H. Wu, "Squeeze film behaviour for porous annular disks", *J. of Lub. Tech.*, vol. 92, 1970, pp. 206-209.
- [3] H. Wu, "An analysis of the squeeze film behavior for porous annular disks", *J. of Lub. Tech.*, vol. 92, pp. 593-596, 1972.
- [4] L. L. Ting, "A Mathematical analog for deformation of porous annular discs squeeze film behaviour including the fluid inertia effect", *J. of Basic Eng.*, vol. 94(2), pp. 417-421, 1972.
- [5] J. Prakash and S. K. Vij, "Load Capacity and Time Height Relation between Porous Plates", *Wear*, vol. 24, pp. 309-322, 1973.
- [6] D. F. Hays, "Squeeze films for rectangular plates", *Trans. ASME*, vol. D. 58, pp.243-251, 1963.
- [7] P. R. K. Murti, "Squeeze Films in curved Circular plates", *Trans. ASME*, vol. F97, pp. 650-652, 1975.
- [8] J. L. Gupta and K. H. Vora, "Analysis of squeeze film between curved annular plates", *J. of Lub. Tech. Trans. ASME*, vol. 102, pp. 48-59, 1980.
- [9] M. B. Ajwalyia, "On certain theoretical aspects of lubrication", *Dissertation*, 1984, Sardar Patel University, Vallabh Vidyanagar.
- [10] R. M. Patel and G. M. Deheri, "Analysis of the squeeze film between curved plates", *J. of Indian acad. of Math.*, vol. 24(2), pp.333-338, 2002.
- [11] P. D. S. Verma, "Magnetic Fluid-Based Squeeze Film", *Int. J. of Eng. Sci.*, vol. 24(3), pp. 305-401, 1986.

- [12] M. V. Bhat and G. M. Deheri, "Squeeze Film Behavior in Porous Annular Disks Lubricated with Magnetic fluid", *Wear*, vol. 151, pp.123-128, 1991.
- [13] M. V. Bhat, *Lubrication with a magnetic fluid*, Team Spirit (India) Pvt. Ltd., 2003, ch 4.
- [14] M. V. Bhat and G. M. Deheri, "Magnetic Fluid-Based Squeeze Film in Curved porous Circular disks", *J. of Mag. and Magn. Materials*, vol. 127, pp. 159-62, 1993.
- [15] R. M. Patel and G. M. Deheri, "Magnetic Fluid-Based Squeeze Film between two curved plates lying along the surfaces determined by secant functions", *Indian J. of Eng. and Material Sci.*, vol. 9, pp. 45-48, 2002.
- [16] J. R. Lin, R. F. Lu and W. H. Liao, "Analysis of magneto-hydrodynamic squeeze film characteristics between curved annular plates", *Indu. Lub. and Tribo.*, vol. 56(50), pp. 300-305, 2004.
- [17] S. T. Tzeng and E. Saibel, "Surface roughness effect on slider bearing lubrication", *Trans. ASLE 10*, pp. 334-342, 1967.
- [18] H. Christensen and K. C. Tonder, "Tribology of rough surfaces: stochastic models of hydrodynamic lubrication", *SINTEF Report No.10/69-18*, 1969a.
- [19] H. Christensen and K. C. Tonder, "Tribology of rough surfaces: parametric study and comparison of lubrication models", *SINTEF Report No.22/69-18*, 1969b.
- [20] H. Christensen and K. C. Tonder, "The hydrodynamic lubrication of rough bearing surfaces of finite width", *ASME-ASLE lubrication conference*, Paper no.70-lub-7, 1970.
- [21] L. L. Ting, "Engagement behaviour of lubricated porous annular disks", *Wear*, vol. 34, pp. 159-182, 1975.
- [22] J. Prakash and K. Tiwari, "Roughness effects in porous circular squeeze-plates with arbitrary wall thickness", *J. of Lub. Tech.*, vol. 105, pp. 90-95, 1983.
- [23] B. L. Prajapati, "Behaviour of squeeze film between rotating porous circular plates: surface roughness and elastic deformation effects", *Pure and Applied Math. Sci.*, vol. 33(1-2), pp. 27-36, 1991.
- [24] S. K. Guha, "Analysis of dynamic characteristics of hydrodynamic journal bearings with isotropic roughness effects", *Wear*, vol. 167, pp.173-79, 1993.
- [25] J. L. Gupta and G. M. Deheri, "Effect of roughness on the behaviour of Squeeze film in a spherical bearing", *Trib. Tran.*, vol. 39, pp 99-102, 1996.
- [26] P. I. Andharia, J. L. Gupta and G. M. Deheri, "Effects of transverse roughness on the behavior of squeeze film in spherical bearings", *Int. J. of Applied Mechanics and Eng.*, vol. 4(1), pp. 19-24, 1999.
- [27] P. I. Andharia, J. L. Gupta and G. M. Deheri, "Effects of surface roughness and hydrodynamic lubrications of slider bearings", *Trib. Tran.*, vol. 44(2), pp. 291-297, 2001.
- [28] J. Prakash and H. Peeken, "The combined effect of surface roughness and elastic deformation in the hydrodynamic slider bearing problem", *Trib. Tran.*, vol. 28(1), pp. 69-74, 1985.
- [29] C. H. Hsu, R. F. Lu and J. R. Lin, "Combined effects of surface roughness and rotating inertia on the squeeze film characteristics of parallel circular disks", *J. of Marine Sci. and Tech.*, vol. 7(1), pp. 60-66, 2009.
- [30] H. C. Patel, G. M. Deheri and R. M. Patel, "Behavior of Squeeze film between rough porous infinitely long parallel plates with porous Matrix of variable film thickness", *Technische Akademie Esslingen, 16th International Colloquium Tribology on Lubrications, Materials and Lub. Engg. C-6, Stuttgart/Ostildern, Germany*, 2008.
- [31] G. M. Deheri, R. M. Patel and N. D. Abhangi, "Magnetic Fluid Based Squeeze Film Behavior between Transversely Rough Curved Plates", *Proceeding of CIST 2008 and ITS-IFTOMM2008, Advanced Tribo.*, Part 3(I), pp.54-55, 2010.
- [32] R. M. Patel, G. M. Deheri and P. A. Vadher, "Magnetic Fluid-Based Squeeze Film between annular plates and transverse surface roughness effect", *ANNALS, Faculty Eng., Hunedoara*, vol. 8 (1), pp. 51-56, 2010.
- [33] G. M. Deheri, R. M. Patel and N. D. Abhangi, "Magnetic fluid-based squeeze film behavior between transversely rough curved annular plates: a comparative study", *Indu. Lub. and Tribo.*, vol. 63(4), pp.254-270, 2011.

G M Deheri, born in 1955, is currently a Reader of Mathematics in the Department of Mathematics Sardar Patel University, Vallabh Vidyanagar, Anand, Gujarat (India). His research interests include Tribology and Functional Analysis.

M E Shimpi, born in 1971, is currently a Associate professor of Mathematics in Birla Vishvakarma Mahavidyalaya Engineering College. Right now, he is a PhD student of Department of Mathematics, Sardar Patel University, Vallabh Vidyanagar, Anand, Gujarat (India). His research interests include Tribology and Functional Analysis.